

Supplementary Information

Intraparticle FRET of Mn(II)-doped Carbon Dots and Its Application in Discrimination of Volatile Organic Compounds

Yu Wang,^a Hu Meng,^a Mingyan Jia,^{a,b} Yu Zhang,^a Hui Li,^a Liang Feng^{*a}

^a Key Lab of Separation Science for Analytical Chemistry,
Dalian Institute of Chemical Physics, Chinese Academy of Sciences,
Dalian, 116023, P. R. China.

^b University of Chinese Academy of Sciences, Beijing 100191, P. R. China

1. Experimental Section

1.1 Materials and apparatus

1-(2-pyridylazo)-2-naphthol (PAN) and manganese chloride tetrahydrate were purchased from Alfa Aesar. Dialysis kits, Pure-A-Lyzer 3500 kDa, was purchased from Sigma Aldrich. All other reagents and solvents were of commercial quality and without further purification. The morphologic study (TEM) of MCDs was performed by using JEM-2100 high-resolution transmission electron microscopy (HRTEM) with 200 kV voltage induced electron beam. UV-Vis absorption spectra were recorded using a Persee TU-1901 UV-Vis spectrophotometer. Fluorescence spectroscopy and 3D emission study were recorded on F-4600 (HITACHI) fluorescence spectrometer. And the fluorescence lifetime experiments were carried out by employing the time-correlated single-photon counting (TCSPC) system on a FluoroMax-4 spectrofluorometer (Horiba Jobin Yvon). Surface enhanced Raman spectrum (SERS) was recorded by using Bruker Optics Senterra R200-L Raman micro-spectrometer ($\lambda=532$ nm, 2 mW). The fluorescence quantum yields of the as-made MCDs in different solvents were determined by comparing the integrated fluorescence intensities and the corresponding absorbance values of quinine sulfate and rhodamine as references.

1.2 Synthesis of MCDs and PCDs

The fabrication of MCDs is according to previous report with a slight modification. To 10 mL ethanol, 49.85 mg of 1-(2-pyridylazo)-2-naphthol and 0.4 mmol of manganese chloride were added and the mixture was stirred for 10 minutes. Then the solution was transferred to a Teflon autoclave. Afterwards, the autoclave was tightly sealed and heated to 180 °C and kept for 4 hours. After reaction, the autoclave was cooled down to room temperature. The product was transferred to 20 mL dialysis kit (3.5 kDa molecular weight cut off, Pure-A-Lyzer, Sigma) and dialyzed in 1.5 L distilled water twice for 48 hour. The as-obtained product was then separated by centrifugation at 12500 rpm (14674 g) for 30 minutes. The supernatant was further purified by filtering with 0.22 μ m filter membrane and then collected as MCDs.

PCDs were fabricated by same synthetic protocol of MCDs only without the addition of manganese chloride salts.

1.3 Nitric acid titration

2 mL of 400 μ g/mL MCDs ethanol solution was transferred to two glass vessel (1 mL for each) and dried in drying oven at 70 °C for 2 hours. After drying, one sample was added with 1 mL of distilled water and the other was firstly added with 900 μ L of distilled water and then 100 μ L of 0.2 M diluted nitric acid. The final concentration of NO_3^- and MCDs in the mixture is 0.02 M and 400 μ g/mL MCDs, respectively. Two solutions were treated with sonication for 20 s before emission spectra recording.

1.4 Sulfur treatment

To 5 mL distilled water, 3 mg MCDs were added and then stirred for 10 minutes before adding 5 mL of 0.06 M Na_2S aqueous solution. The mixture was kept stirring for 1 hour and transferred to 20 mL dialysis kit (3.5 kDa molecular weight cut off, Pure-A-Lyzer, Sigma). The dialysis was made against 1 L distilled water for 24 hours with water-refreshing twice. After dialysis, the mixture was purified with centrifugation at 12500 rpm (14674 g) for 30 minutes. The supernatant was further purified by filtering with 0.22 μ m filter membrane and then collected as S^{2-} -treated MCDs. S^{2-} -treated PCDs were obtained by employing the same protocol.

1.5 Preparation for SERS

Samples were prepared according to the previous literature with slight modification. Briefly, glass slides were cut into 10 mm × 10 mm and washed with diluted nitric acid and distilled water for several times. The clear slides were then frosted before further use. Tollen's reagent was prepared in a small beaker by adding about 10 drops of fresh 5% NaOH solution to 10 mL of 2-3% AgNO₃ solution, where upon a dark-brown AgOH precipitate was formed. This step was followed by dropwise addition of concentrated NH₄OH, at which point the precipitate re-dissolved. The beaker containing the clear Tollen's reagent was then placed in ice bath. The frosty slides were placed into beaker. 3 mL of 10% D-glucose was added into the beaker with careful swirling to ensure mixing. The beaker was then removed from the ice bath and kept for 30 minutes to room temperature. The beaker was placed into water bath (55°C) for 1 min followed by sonication for one minute. Finally, the silver-coated slides were rinsed several times with distilled water and sonicated again in distilled water for 30 s. The slides were then stored in distilled water for several hours prior to exposure to the adsorbate solution. At last, the slides were air-dried and then dipped into 12 mg/mL MCDs ethanol solution. The slides were in contact with the solution for at least 1 hours before air drying.

1.6 VOCs vapors discrimination

The MCDs powder was dispersed in EtOH to gain different MCDs stock solutions at different concentrations, including 3.2, 1.6, 0.8, 0.4, 0.2 and 0.1 mg/mL. The stock solutions were then equably loaded into a 6-hole Teflon ink well (3 x 2) printed on a thin PVDF film in sequence of concentration (which delivered approximately 1 µL for each well). The film was dried in oven for 48 hours. In order to obtain saturated vapor, the organic solvent was fully added to a 20 mL glass vial and heated to its boiling point. The detection was conducted in an open-air condition where the temperature was kept at 20°C with 30% relative humidity. After solvent boiling, the PVDF-MCDs film was placed above the bottleneck and held for 3 s, and then dried for 10 s before exposing to a 365 nm UV lamp. The difference map was achieved by subtracting before and after exposure images. The color ranges of difference map is expanded from four to eight bit per color (red, green and blue range of 2-25 expanded to 0-255).

1.7 Calculation of extinction coefficient

The molar absorptivity of MCDs in different solvents was calculated by employing Beer-Lambert Law, the equation is given as follow:

$$A = \varepsilon cl$$

Where A is absorbance (no units) measured from absorption spectrum, ε is the extinction coefficient ((g/L)⁻¹ cm⁻¹), c is the concentration of MCDs in solvent (mg L⁻¹), l is path length of the sample (cm).

1.8 Calculation of relative QY of MCDs

The relative fluorescence quantum yield (QY) of MCDs was calculated by linearizing integrated fluorescence intensities (excitation at 350 nm for samples in cyclohexane, toluene, 1,4-dioxane and chloroform; at 488 nm for samples in methylene chloride, acetone, acetonitrile, ethanol, methanol, glycol and distilled water) of MCDs and reference (quinine sulfate $\Phi=0.58$ for samples in cyclohexane, toluene, 1,4-dioxane and chloroform; rhodamine 6G $\Phi=0.95$ for samples in methylene chloride, acetone, acetonitrile, ethanol, methanol, glycol and distilled water) versus

their corresponding absorbance. The absorbance intensities of all samples were determined by using UV-Vis spectrometer and were kept below 0.1 in order to minimize re-absorption effects. The emission intensity of MCDs and reference were probed at the same excitation wavelength. Then the QY was calculated using the following equation for calculation of QY is:

$$\Phi_X = \Phi_{ST} \times \left(\frac{I_X}{I_{ST}} \right) \times \frac{A_{ST}}{A_X} \times \frac{\eta_X^2}{\eta_{ST}^2}$$

where I is the integrated emission intensity, η is the refractive index of the solvent, A is the absorbance, Φ is the QY, X stands for MCDs, ST refers to rhodamine 6G or quinine sulfate. Thereamong, rhodamine 6G was dissolved in deionized water (refractive index: 1.33) while quinine sulfate was dissolved in 0.1 M H_2SO_4 . The MCDs were dissolved in deionized water (refractive index: 1.33).

1.9 Relationship between ϵ and E deduced from Equations

$$\phi = \frac{\Gamma}{\Gamma + k_{nr}} \quad (1)$$

$$\tau = \frac{1}{\Gamma + k_{nr}} \quad (2)$$

In equation 1, ϕ is quantum yield. k_{nr} is non-radiation rate of fluorophore. Γ is the emissive radiation rate of fluorophore. τ is lifetime of a fluorophore. ϕ_D and τ_D are intrinsic parameters for a certain fluorophore, which means if without other exterior influences ϕ would associate to τ with a direct ratio. This ratio is called intrinsic or natural lifetime, as shown in equation 3.

$$\tau_n = \frac{\tau}{\phi} \quad (3)$$

At the meantime, in a classical FRET system, FRET rate k_{FRET} can be calculated as:

$$k_{FRET} = \frac{\phi_D \kappa^2}{\tau_D r^6} \left(\frac{9000 \ln(10)}{128 \pi^5 N n^4} \right) J(\lambda) \quad (4)$$

ϕ_D refers to relative quantum yield of donor. κ^2 is a factor describing the relative orientation in space of the transition dipoles of the donor and acceptor. τ_D is fluorescence lifetime of donor in the absence of acceptor. r is the distance between donor and acceptor. N is Avogadro's number. n is the refractive index. The overlap integral $J(\lambda)$ expresses the degree of spectral overlap between the donor emission and the acceptor absorption.

When bring equation 3 into equation 4, the FRET rate k_{FRET} is

$$k_{FRET} = \text{constants} \frac{\kappa^2}{\tau_n r^6 n^4} J(\lambda) \quad (5)$$

In MCDs, τ_n is an intrinsic parameter of donor while n is solvent reflection. κ^2 is assigned to be 2/3 due to the random rotation between FE and ME. Comparing to molecular FRET pairs, spatial distribution of FE and ME are much confined due to their intrinsic immobilization at few-layered carbon backbone (approximate 1 nm in thickness from AFM spectrum according to previous work) which is derived from large conjugated rigid precursors PAN and plane configuration of PAN-Mn complex. Thus, if r is fluctuated in a very limited range, then $J(\lambda)$ will play a larger part in calculation of k_{FRET} .

At the meantime, $J(\lambda)$ can be calculated as:

$$\int_0^\infty J(\lambda) = \frac{\int_0^\infty F_D(\lambda) \epsilon_A(\lambda) \lambda d\lambda}{\int_0^\infty F_D(\lambda) d\lambda} \quad (6)$$

$$E = \frac{k_{FRET}}{\tau_D^{-1} + k_{FRET}} \quad (7)$$

F_D is the fluorescent intensity of donor, ϵ_A is the extinction coefficient of acceptor, λ is wavelength. According to equation 6, it can be seen that a large ϵ_A will lead to a large $J(\lambda)$, and give rise to a fast k_{FRET} . According to equation 7, fast k_{FRET} will make FRET more efficient.

Thus, in the case of MCDs, large ϵ_A of ME will directly lead to high efficiency of IPFRET, as

$$\epsilon_{ME} \propto J(\lambda) \propto k_{FRET} \propto E$$

2. Figures and Tables

Table S1. IPFRET of MCDs in Tol-Ace binary mixture

Ace Fraction (%)	$E_N^{T^s}$	Emission (nm)	Excitation (nm)	Transition energy (ΔE , eV)	Extinction coefficient (ϵ , (g/L)-1 cm-1)
10	0.212	445	330	2.94	0.41
20	0.228	445	334	2.95	0.48
30	0.240	446	340	2.96	0.89
40	0.259	544	341	2.97	1.26
50	0.274	545	350	2.97	1.49
60	0.287	544	452	2.97	1.88
70	0.308	544	450	2.98	2.15
80	0.327	544	447	2.98	2.37
90	0.342	541	445	2.99	2.52

Table S2. IPFRET of MCDs in different solvents.

Solvents	E_T^N	Emission (nm)	Excitation (nm)	Transition energy (ΔE , eV)	Extinction coefficient (ϵ , (g/L) ⁻¹ cm ⁻¹)	Quantum yield(Φ) ^a
Cyclohexane	0.006	408	287	3.1	0.34	2.04
Toluene	0.099	413	297	2.99	0.53	12.23
1,4-dioxane	0.164	441	317	2.97	1.54	5.71
Chloroform	0.259	441	339	2.95	1.64	4.63
MC	0.309	541	341	2.97	2.21	20.98
Acetone	0.355	550	444	2.99	2.53	19.25
Acetonitrile	0.46	551	444	3.00	2.54	17.16
EtOH	0.654	577	452	3.01	2.67	4.37
MeOH	0.762	574	446	3.02	2.68	4.60
Glycol	0.79	578	447	3.03	2.59	6.82
H ₂ O	1	567	443	3.08	1.79	4.23

^a: Quantum yields of Cyc, Tol, Dio and Chl are calculated according to quinine sulfate in 0.1 M H₂SO₄, others are calculated by using rhodamine 6G as a reference

Table S3. TCSPC analyses of MCDs

Solvent	<i>Em.440</i>				<i>Em.560</i>			
	$\tau_1(\text{ns})$ /	$\tau_2(\text{ns})$ /	$\tau_3(\text{ns})$ /	$\tau_{\text{avg.}}(\text{ns})$	$\tau'_1(\text{ns})$ /	$\tau'_2(\text{ns})$ /	$\tau'_3(\text{ns})$ /	$\tau_{\text{avg.}}(\text{ns})$
	prop.(%)	prop.(%)	prop.(%)		prop.(%)	prop.(%)	prop.(%)	
Toluene	0.46 / 29.32	-	3.45 / 70.68	2.57	7.33×10^{-3} / 7.95	0.46 / 87.31	3.90 / 4.74	0.56
Acetonitrile	0.26 / 21.25	2.20 / 41.24	5.89 / 37.52	3.17	-	0.10 / 4.34	10.10 / 95.66	9.68
Glycol	0.89 / 32.23	2.50 / 42.84	7.17 / 24.93	3.15	8.97×10^{-2} / 3.89	3.59 / 82.41	5.66 / 13.69	3.74
H ₂ O	0.11 / 9.88	2.90 / 17.37	9.01 / 72.75	7.07	7.41×10^{-2} / 24.66	2.86 / 71.04	11.60 / 4.31	2.55

Table S4. Vapor pressures at Boiling point of 10 solvents.

Analyte	Boiling point (°C)	Vapor Pressure (25 °C, ppmv) ^a
Cyclohexane	80.4	146000
Toluene	110.6	36000
1,4-Dioxane	101.1	44000
Chloroform	61.2	263000
Acetone	56.53	340000
Acetonitrile	81.1	112000
Ethanol	78.4	78000
Methanol	64.7	170000
Ethylene glycol	197.3	550
Water	100	36000

^a Vapor pressures from the Material Safety Data Sheets (MSDS). Due to differences among sources and small variations in temperatures, these values should be taken as approximate only.

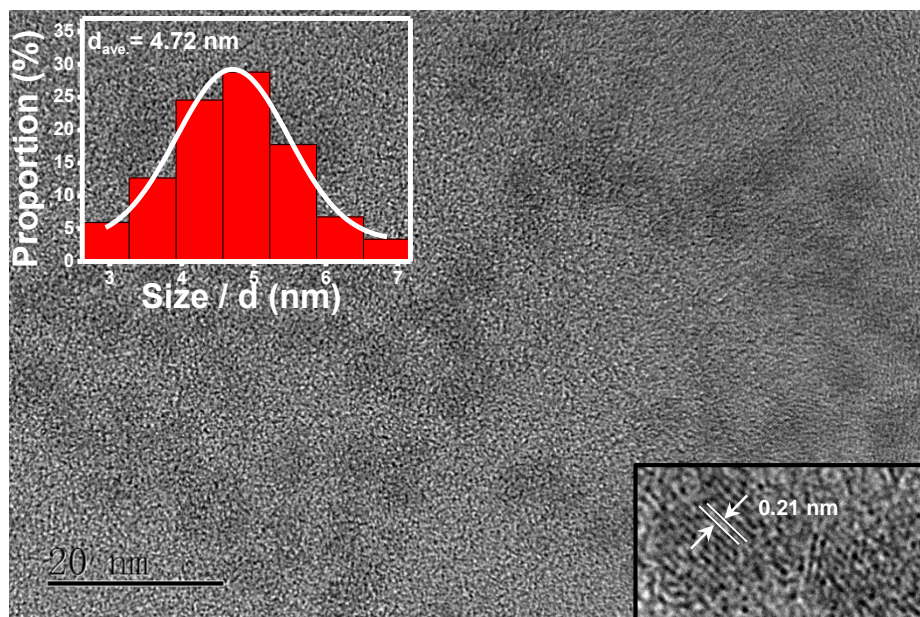


Figure S1. TEM of MCDs, the size distribution analysis indicate the size of MCDs exhibit a relatively small fluctuation with the average value of 4.72nm.

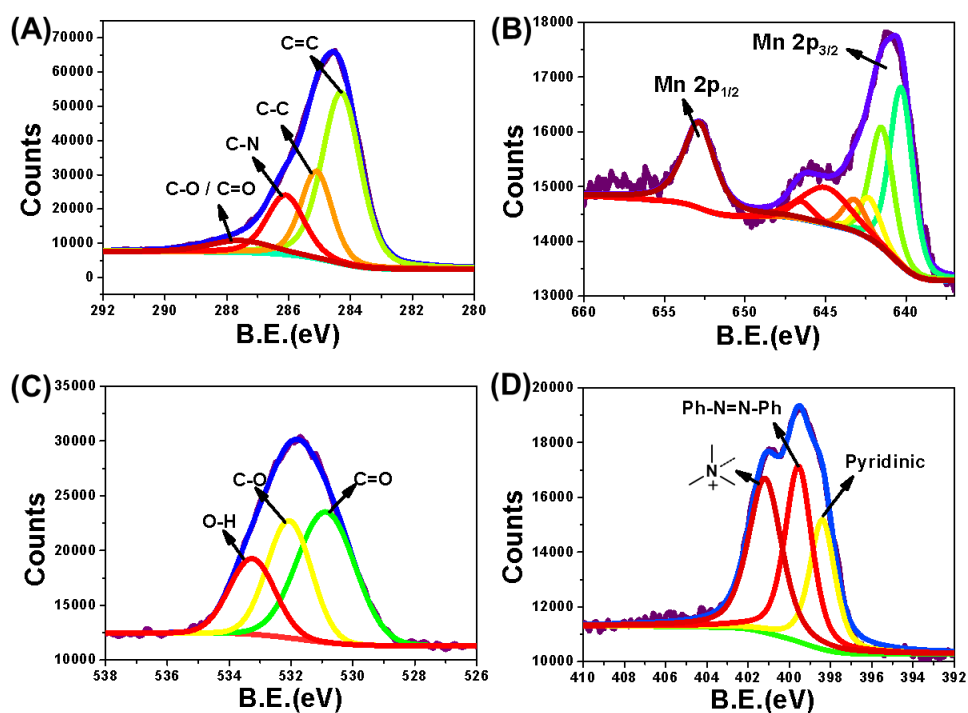


Figure S2. X-ray photoelectron spectroscopy of MCDs

XPS survey data (atomic percentage) for the elements.

Peak designation	Band (eV)	At. % conc.	FWHM (eV)
C 1s	284.61	76.18	2.27
O 1s	531.74	10.76	3.20
Cl 2p	198.40	2.75	3.65
N 1s	399.45	9.37	4.05
Mn 2p	641.22	0.94	3.43

Notes:

X-ray photoelectron spectroscopy (XPS) spectra uncover the existence of Mn(II)-coordination in MCDs. Firstly, Mn 2p spectra (Figure 2a) partially resemble those of MnO, proving that the coordination of Mn•••O exists. It is noteworthy that Mn•••O coordinating peak does not appear in O 1s spectra (Figure 2b), implying extremely few oxygen atoms participate into the coordination, which agrees well with the low absolute content of Mn (< 1 At. %) in MCDs (see the table above). In other words, if the coordination occurs at the surface oxygen groups, more Mn²⁺ would be captured during the fabrication since the addition of Mn²⁺ is excessive in molar reactant ratio (PAN : Mn²⁺ = 1:2). Thus, the oxygen atom participated in the Mn•••O coordination is more likely supplied by PAN-derived naphtholic oxygen, indicating that Mn-coordination can remain in the controlled carbonization. In addition, extremely small content of Mn(II) suggests MCDs would be with restrained cytotoxicity.

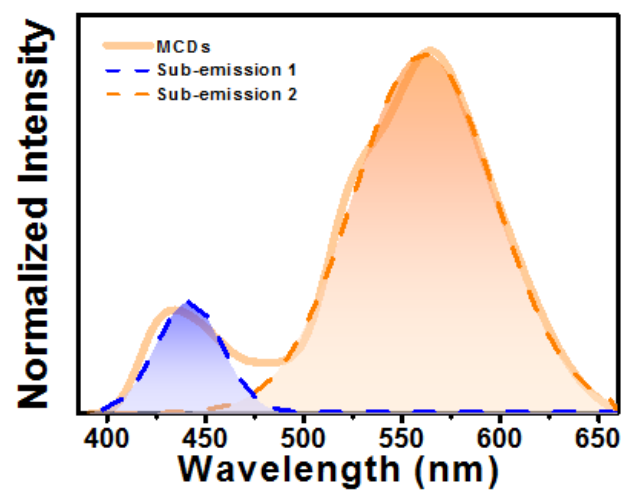


Fig. S3. Emission spectrum of MCDs in DW.

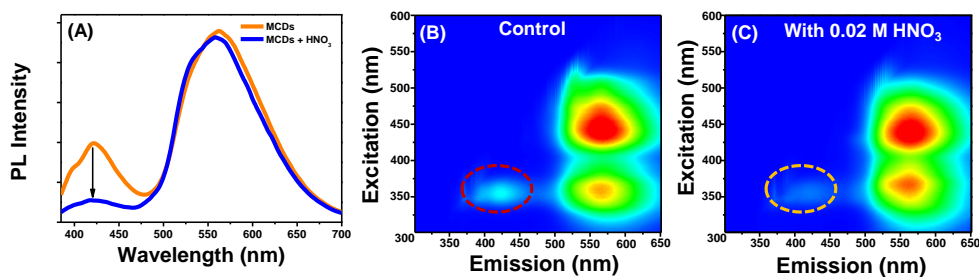


Fig. S4. (A) Fluorescence spectroscopy of 400 $\mu\text{g/mL}$ MCDs in distilled water before and after the addition of 0.02 M HNO_3 at 365nm excitation. (B) and (C) are 2D fluorescence spectra, which demonstrate the variation of two sub-emission before and after protonation.

Notes:

It has been widely reported that fluorescence of common CDs ranging from 400 to 500 nm is originated from structures involving -C=O .¹⁻⁴ In the case of our MCDs, plenty of C=O with negligible carboxylic groups are detected according to X-ray photoelectron spectroscopy (see the Appendix, Fig. A4). Theoretically, structure of emission center that with C=O groups can be protonated easily, and consequentially leads to noticeable spectral variation. Such experiment has been much in studies of conventional CDs.³⁻⁵ Hence, we compared the two-dimensional fluorescence spectroscopy of MCDs recorded before and after adding diluted nitric acid, as shown in Fig. S2 A-C. After protonation, sub-emission around 440 nm was almost vanished, whereas sub-emission centered at 567 nm was influenced finitely. This result can give a semi-empirical conclusion that the protonation-sensitive sub-emission in short wavelength region may mainly correlate to FE.

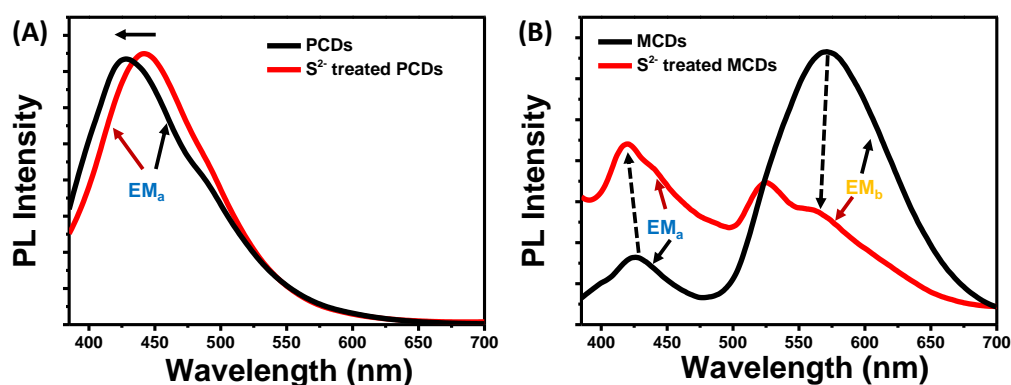


Fig. S5. S²⁻-treatment for MCDs and PCDs.

Notes:

In order to investigate whether manganese cation is participating in emission of MCDs, we tried to interfere the functionality of Mn(II)-coordination by adding excess amounts of S²⁻ to MCDs aqueous solution since sulfide ion has been extensively used for extraction of heavy metal cations.⁶ A simple trial was performed by applying S²⁻-treatment to both Mn(II)-free PCDs and Mn(II)-doped MCDs. As shown in Fig. S3A, only sub-emission with a short wavelength (EM_a) was observed for PCDs. After treated with S²⁻, the EM_a only showed a feeble blue-shift without obviously quenching or band-generating, indicating that S²⁻-treatment finitely affected EM_a. However, by employing S²⁻-treatment to MCDs, dramatic changes were observed by comparing the emission spectra with untreated ones, as shown in Fig. S3B. The sub-emission band in the long-wavelength region substantially dropped down, indicating that crucial interaction took place at this emissive center. Deductively, the weakened EM_b can be assigned to metal-correlated emission (ME).

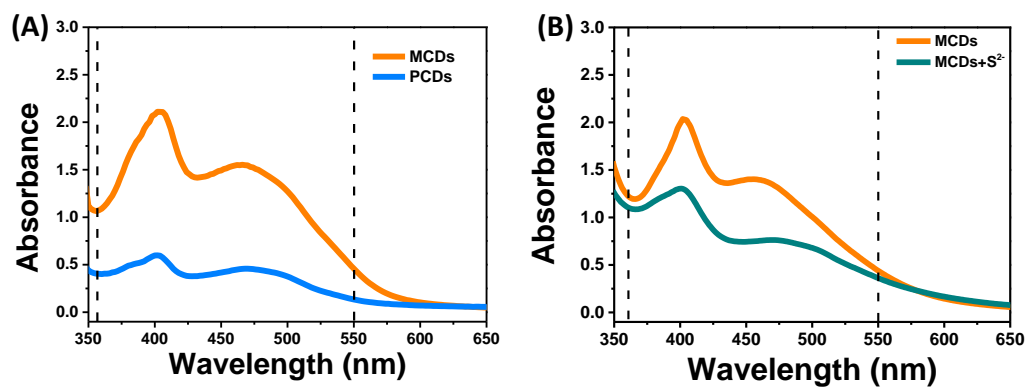


Fig. S6. (A) Absorption spectra of MCDs and PCDs; (B) Absorption spectra of MCDs before and after S²⁻-treatment.

Notes:

By doping with metal ions, the absorption band range from 360 nm to 550 nm is much strengthened, corresponding to metal-related charge transfer transition.⁷ And upon the addition of metal extraction agent sodium sulfide, this band was found much weakened, confirming its origin from metal-based component.

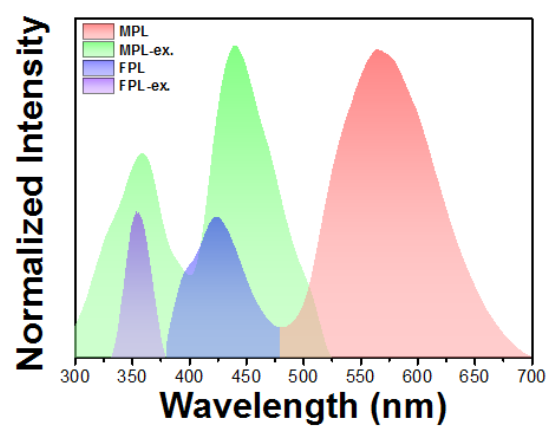


Fig. S7. Illustration for energy transfer in MCDs.

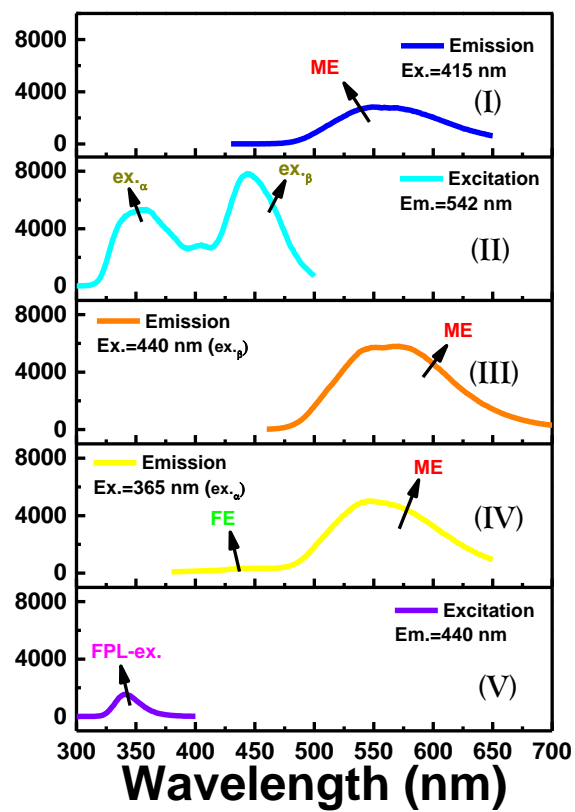


Fig. S8. Spectral investigation of MCDs in Ace

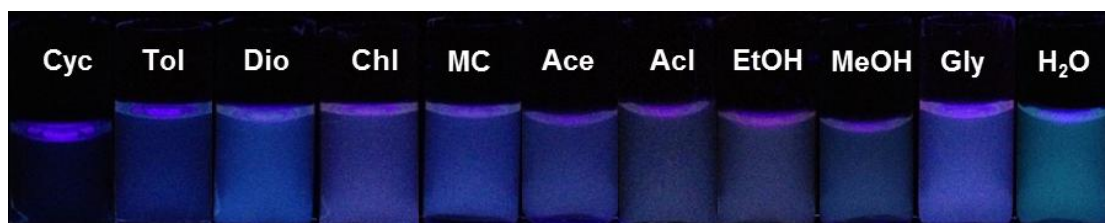


Fig. S9. Fluorescence of PCDs in different solvents. The solvents: Cyc: cyclohexane, Tol: toluene, Dio: 1,4-dioxane, Chl: chloroform, MC: methylene chloride, Ace: acetone, Acl: acetonitrile, EtOH: ethanol, MeOH: methanol, Gly: glycol and DW: distilled water.

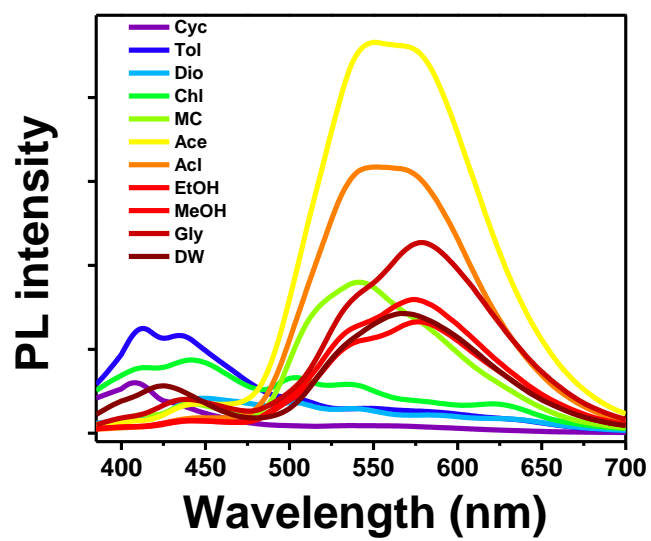


Fig. S10. Emission spectra of MCDs in different solvents at 365 nm excitation.

3. References

1. Zhu, S.; Zhang, J.; Tang, S.; Qiao, C.; Wang, L.; Wang, H.; Liu, X.; Li, B.; Li, Y.; Yu, W.; Wang, X.; Sun, H.; Yang, B. *Adv. Func. Mater.* **2012**, *22*, 4732-4740.
2. Wang, L.; Zhu, S.-J.; Wang, H.-Y.; Qu, S.-N.; Zhang, Y.-L.; Zhang, J.-H.; Chen, Q.-D.; Xu, H.-L.; Han, W.; Yang, B.; Sun, H.-B. *Acs Nano* **2014**, *8*, 2541-2547.
3. Bao, L.; Zhang, Z.-L.; Tian, Z.-Q.; Zhang, L.; Liu, C.; Lin, Y.; Qi, B.; Pang, D.-W. *Adv. Mater.* **2011**, *23*, 5801-5806.
4. Zheng, H.; Wang, Q.; Long, Y.; Zhang, H.; Huang, X.; Zhu, R. *Chem. Comm.* **2011**, *47*, 10650-10652.
5. Zhu, S.; Song, Y.; Zhao, X.; Shao, J.; Zhang, J.; Yang, B. *Nano Research* **2015**, *8*, 355-381.
6. Peters, R. W.; Shem, L. *Separation of Heavy-Metals-Removal from Industrial Wastewaters and Contaminated Soil* **1993**; 3-64.
7. Vekshin, N. L. *Energy Transfer in Macromolecules*. SPIE Press: 1996.